Searches for the Higgs boson into fermions at ATLAS

Victoria J. Martin, On behalf of the ATLAS Collaboration.
School of Physics and Astronomy, University of Edinburgh, Edinburgh, EH9 3JZ, United Kingdom

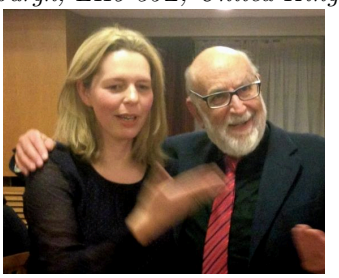

The discovery of a Higgs-like boson by the ATLAS Collaboration at the LHC relies on evidence from di-boson decays: $\gamma\gamma$, ZZ^* and WW^*. The Standard Model predicts that the Higgs boson with $m_H \sim 125$ GeV should also have significant branching ratios to pairs of bottom and charm quarks, tau-leptons and muons. Decays to these final states are significantly more challenging to detect due to large backgrounds and the requirement to search for associated production of the Higgs boson. These proceedings review searches from ATLAS for the Standard Model Higgs boson (H) into fermions: $H \to \tau^+\tau^-$, $H \to \mu^+\mu^-$, $H \to b\bar{b}$, in association with top-quark pairs and vector bosons and into invisible final states, $H \to$ invisible, using up to 4.7 fb^{-1} of $\sqrt{s} = 7$ TeV and up to 21 fb^{-1} of $\sqrt{s} = 8$ TeV proton-proton collision data from the LHC. No observation of events above backgrounds expectations is observed in any of the searches. Limits are set on the Higgs boson production in the mass range 100 GeV $< m_H <$ 150 GeV.

ATL-PHYS-PROC-2013-208
26/07/2013

1 Introduction

The search for the Standard Model Higgs boson (H) – as predicted by the Brout-Englert-Higgs mechanism [1,2,3,4] – has been one of the highest priorities of the field of particle physics. The observation of a boson of mass around 125 GeV decaying to a pair of photons and into massive vector bosons was reported last year by the ATLAS [6] and CMS [7] Collaborations at the LHC. Measurements from the CDF and DØ Collaborations at the Fermilab Tevatron also provide evidence for production of a particle with mass of around 125 GeV [8].

The Higgs boson is predicted to interact with weak gauge bosons (W, Z), with fermions via the Yukawa interaction, and also undergo triple and quartic self-interactions. A Standard Model Higgs boson of mass $m_H \sim 125$ GeV is predicted to decay most frequently into fermions. The predicted branching ratios of the Higgs into fermions are given in Table 1 [9].

1.1 Notation

Throughout these proceedings, V represents a W- or Z-boson, ℓ represents an electron or muon (of either charge) and j represents a hadronic jet. The symbol τ_{had} represents the hadronic decay of the τ-lepton: $\tau \to$ hadrons $+ \nu_\tau$ and τ_{lep} represents the leptonic decay of the τ-lepton: $\tau \to \ell\nu_\ell\nu_\tau$. σ_{SM} is the Standard Model production cross section of the process being discussed.

Table 1: Predicted branching ratios for the Standard Model Higgs boson, with $m_H = 125$ GeV, into fermions. Numbers taken from reference [9].

Decay mode	Branching ratio (%)
$H \to b\bar{b}$	57.7 ± 1.9
$H \to c\bar{c}$	2.9 ± 0.4
$H \to \tau^+\tau^-$	6.3 ± 0.4
$H \to \mu^+\mu^-$	0.022 ± 0.001

2 The LHC Environment

Searches for Higgs boson production at the LHC are challenging due to a very large total cross section. The main backgrounds to the searches presented in these proceedings come from QCD b-jet production and Drell-Yan production to muon and tau pairs. These backgrounds have production cross sections of around 10^7 and 10^5 times larger, respectively, than direct Higgs boson production.

In order to increase the sensitivity of the searches and to reduce backgrounds, the analyses presented here exploit associated Higgs boson production through vector boson fusion: $pp \to jjVV \to jjH$, with top-quarks: $pp \to t\bar{t}H$ or with W or Z bosons: $pp \to WH$, $pp \to ZH$.

2.1 Tau-lepton and b-jet Identification

In the search for fermionic final states of the Higgs boson, key analysis techniques include the identification of b-quarks and hadronically decaying τ-leptons [10].

Around 65% of τ-leptons decay hadronically; jets and tracks are used to identify these τ_{had} candidates. The energy of such candidates is reconstructed using Monte Carlo information calibrated using isolated hadron data. The analyses presented in these proceedings use the so-called "60% working point" that selects 60% of τ_{had} candidates, and only a few percent of QCD jets and less than one percent of electrons.

The identification of b-jets relies on the reconstruction of secondary and subsequent vertices along the b-hadron's line of flight. The analyses presented in these proceedings use the so-called "70% working point" that selects 70% of b-jets and has mistag rate of around 1% for light-quark jets and around 20% for c-jets.

3 Searches for $VH \to Vb\bar{b}$ Production

The aim of the $VH \to Vb\bar{b}$ search is to identify the Higgs boson decaying into a pair of b-jets in association with a W- or Z-boson. As presented in Table 2, the search uses the leptonic final state of the W- or Z-boson, requiring either exactly zero, one or two charged leptons with exactly two or three reconstructed high transverse momentum (p_{T}) jets; two of the jets must be b-tagged [11]. To improve sensitivity, the analysis is performed in bins of vector boson p_{T}; in total 16 exclusive search regions are used in the search. In each region, the reconstructed di-b-jet mass, $m_{b\bar{b}}$, is used as the discriminating variable.

Figure 1 shows the observed $m_{b\bar{b}}$ distribution in the most sensitive search regions. The shape of the signal and of each of the predicted backgrounds is also shown.

3.1 Backgrounds and Systematic Uncertainties

The main backgrounds to the search for $VH \to Vb\bar{b}$ production come from top-quark production, and W+jets and Z+jets production. The shape of these backgrounds in each of the search regions are taken from Monte Carlo simulations and normalised using data. The shape of QCD

Table 2: Search categories for the $VH \to Vb\bar{b}$ analysis [11]. $E_{\mathrm{T}}^{\mathrm{miss}}$ is the scalar sum of the missing momentum transverse to the beam, $m_{\ell\ell}$ is the invariant mass of the two charged leptons and $m_{\mathrm{T}}^{\ell\nu}$ is the "transverse mass" of the charged lepton and the missing momentum. The transverse mass can be defined as $(m_{\mathrm{T}}^{\ell\nu})^2 = E_{\mathrm{T}}^{\ell} E_{\mathrm{T}}^{\nu} - \vec{p_{\mathrm{T}}}^{\,\ell} \cdot \vec{p_{\mathrm{T}}}^{\,\nu}$.

zero lepton $ZH \to \nu\bar{\nu}b\bar{b}$	one lepton $WH \to \ell\nu b\bar{b}$	two lepton $ZH \to \ell^+\ell^- b\bar{b}$
No electrons or muons	exactly one high-p_{T} lepton	exactly two high-p_{T} leptons opposite charge
$E_{\mathrm{T}}^{\mathrm{miss}} > 120$ GeV	$E_{\mathrm{T}}^{\mathrm{miss}} > 25$ GeV 40 GeV $< m_{\mathrm{T}}^{\ell\nu} < 120$ GeV	$E_{\mathrm{T}}^{\mathrm{miss}} < 60$ GeV 83 GeV $< m_{\ell\ell} < 99$ GeV

multi-jet production is determined by data-driven techniques. Irreducible background from $WZ(Z \to b\bar{b})$ and $ZZ(Z \to b\bar{b})$ production is normalised to the predicted Standard Model cross section.

The main systematic uncertainties in the search come from b- and c-jet tagging, the jet energy scale, and from the limited statistics of the Monte Carlo samples. Systematic uncertainties are constrained by fitting signal and background templates of the $m_{b\bar{b}}$ distribution, derived from Monte Carlo simulations, to the observed data in signal regions and several background-dominated control regions.

No excess of data events, compared to expectations from backgrounds, is observed. Therefore limits are set on the ratio of the measured cross section for $VH \to Vb\bar{b}$ compared to the Standard Model expectation: $\sigma(VH \to Vb\bar{b})/\sigma_{\mathrm{SM}} < 1.8$ (1.9 expected) for $m_H = 125$ GeV at 95% confidence level. The limits as a function of the Higgs boson mass are shown in Figure 8.

3.2 Observation of $VZ \to Vb\bar{b}$ Production

The analysis technique is validated by searching for $VZ \to Vb\bar{b}$ production, which has a very similar signature, but a predicted cross section around five times larger than $VH \to Vb\bar{b}$ production. Figure 2 shows the $m_{b\bar{b}}$ distribution with all backgrounds, except VZ and VH production, subtracted. A clear peak in the observed events around 90 GeV can be seen. An independent fit to the data is made, fixing the value of the Higgs boson production to the Standard Model prediction. The fit results in an observation of $VZ \to Vb\bar{b}$ production with $\sigma(VZ \to Vb\bar{b})/\sigma_{\mathrm{SM}} = 1.09 \pm 0.20(\mathrm{stat}) \pm 0.22(\mathrm{syst})$, corresponding to a observation with a significance of 4.0 standard deviations.

4 Search for $ZH, H \to$ invisible Production

Although not predicted by the Standard Model with an appreciable rate, it is instructive to search for possible invisible decays of the Higgs boson. At ATLAS, the search for invisible Higgs boson production uses associated production with a leptonically decaying Z-boson [12]. The signature is $Z \to \ell^+\ell^-$ with large missing transverse momentum, $E_{\mathrm{T}}^{\mathrm{miss}} > 90$ GeV. The main backgrounds to the search come from diboson production: $ZZ \to \ell^+\ell^-\nu\bar{\nu}$ (70%), $WZ \to \ell\nu\ell^+\ell^-$ – where one charged lepton escapes detection – (20%) and $WW \to \ell^+\nu\ell^-\bar{\nu}$ (5%).

The event selection is optimised to select signal-like events. The number of observed events, and the number of expected background events are shown in Table 3. No excess of data events is observed. The results are interpreted in two ways: a limit is set on the branching ratio of $H \to$ invisible for a Standard Model Higgs boson of $m_H = 125$ GeV of $< 65\%$ at 95% confidence level (to be compared with an expected limit of $< 84\%$ at 95% confidence level). The limits for different Higgs boson masses are shown in Figure 3. Secondly a limit on the cross section times branching ratio, $\sigma(ZH) \cdot \mathrm{BR}(H \to \mathrm{invisible})$, of further Higgs-like states in the range 115 GeV $< m_H <$ 300 GeV is derived, as shown in Figure 8.

Figure 1: The di-b-jet mass distribution in different search regions from the $\sqrt{s} = 8$ TeV dataset used in the search for $VH, H \to b\bar{b}$ production, from reference [11]. Top: for search regions with zero charged leptons; middle: for search regions with one charged lepton; bottom: for search regions with two charged leptons.

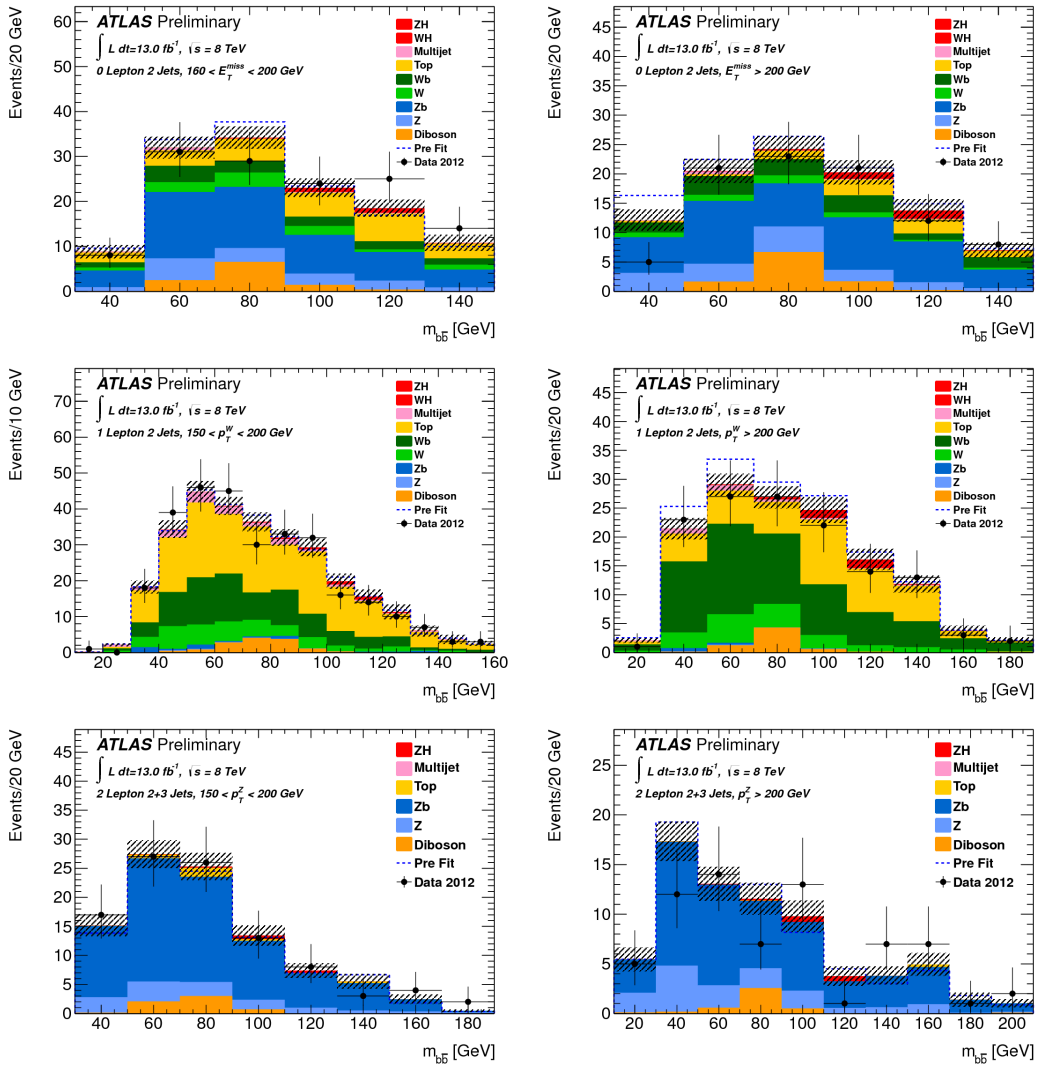

Figure 2: Background subtracted di-b-jet mass distribution, compared to predicted shapes, taken from reference [11]. The peak at $m_{b\bar{b}}$ is evidence for $Z \to b\bar{b}$ production in association with the W- or Z-boson.

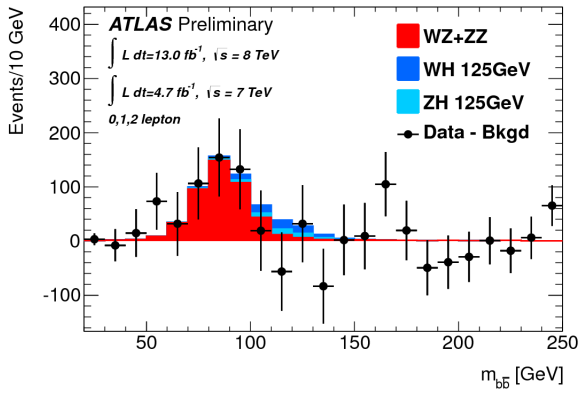

Table 3: Number of expected background and observed events for the $H \to$ invisible search [12].

	expected SM background for $m_H = 125$ GeV	observed events
$\sqrt{s} = 7$ TeV, 4.7 fb^{-1}	$32.7 \pm 1.0(\text{stat}) \pm 2.6(\text{syst})$	27
$\sqrt{s} = 8$ TeV, 13.0 fb^{-1}	$78.0 \pm 2.0(\text{stat}) \pm 6.5(\text{syst})$	71

Figure 3: Results from the search for $ZH, H \to$ invisible production, taken from reference [12]. Left: the missing transverse momentum distribution after an optimised event selection. The area denoted by the dashed line corresponds to the events expected if the branching ratio for $H \to$ invisible is 100%. Right: resulting limits on the cross section times branching ratio of a Higgs-like boson into invisible final states. The red dotted line shows σ_{SM} for ZH production with $Z \to \ell^+\ell^-$ and $H \to$ invisible, assuming a branching ratio for $H \to$ invisible of 100%.

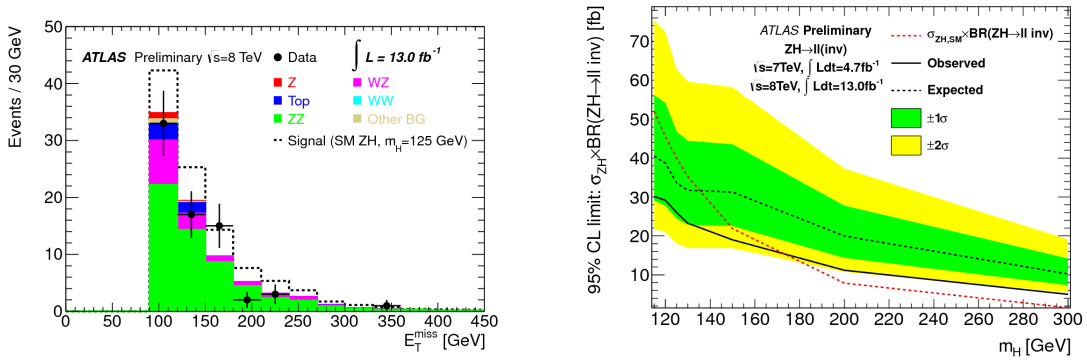

5 Searches for $t\bar{t}H, H \to b\bar{b}$ Production

The production of $t\bar{t}H$ with $H \to b\bar{b}$ results in a complex final state, containing the decay products of both the Higgs boson and the two top quarks. This search [13] uses the "single-lepton" final state where one of the W-bosons, produced from the decay of a top quark, decays into an electron or muon plus a neutrino, and the other W-boson decays hadronically. The final state therefore consists of one charged lepton, six jets – of which four are b-jets – and missing transverse momentum.

For events with at least six reconstructed jets, and at least three b-tags, a kinematic likelihood fitter is used to reconstruct the W-bosons and top quarks. The fitter employs knowledge of particle decay widths and detector resolutions to identify the best assignment of the reconstructed jets, lepton and missing transverse momentum to the W-boson and top quarks. The invariant mass of the two remaining jets, $m_{b\bar{b}}$, is then considered as the Higgs candidate mass and is used as the discriminating variable.

Events with less than six reconstructed jets, or less than three b-tags, are also used in the analysis to improve sensitivity and constrain backgrounds. In these regions, $H_{\text{T}}^{\text{had}}$, the scalar sum of the jet-p_{T}, is examined.

The main background to the search comes from $t\bar{t}$ production and the main systematic uncertainties are due to b-jet and c-jet tagging. The systematic uncertainties and background contributions are constrained by fitting the $m_{b\bar{b}}$ and $H_{\text{T}}^{\text{had}}$ distributions. Figure 4 shows the invariant di-b-jet mass before and after the fit to the observed data is performed.

Using 4.7 fb^{-1} of data at $\sqrt{s} = 7$ TeV, no deviation from Standard Model backgrounds is observed. Therefore a limit is set on $\sigma(t\bar{t}H, H \to b\bar{b})/\sigma_{\text{SM}}$ at 95% confidence level of 13.1 for $m_H = 125$ GeV. The expected limit for the dataset used in the search is 10.5 at 95% confidence level.

Figure 4: Di-b-jet mass distributions from the $t\bar{t}H, H \to b\bar{b}$ search, taken from reference [13]. The upper plots show events with at least six high-p_{T} jets of which exactly three are b-tagged; the lower plots show events with at least six high-p_{T} jets of which exactly four or more are b-tagged. Plots on the left show the distributions before the fit; plots on the right show the distributions after the fit. The data points are the same on the left- and right-hand-sides.

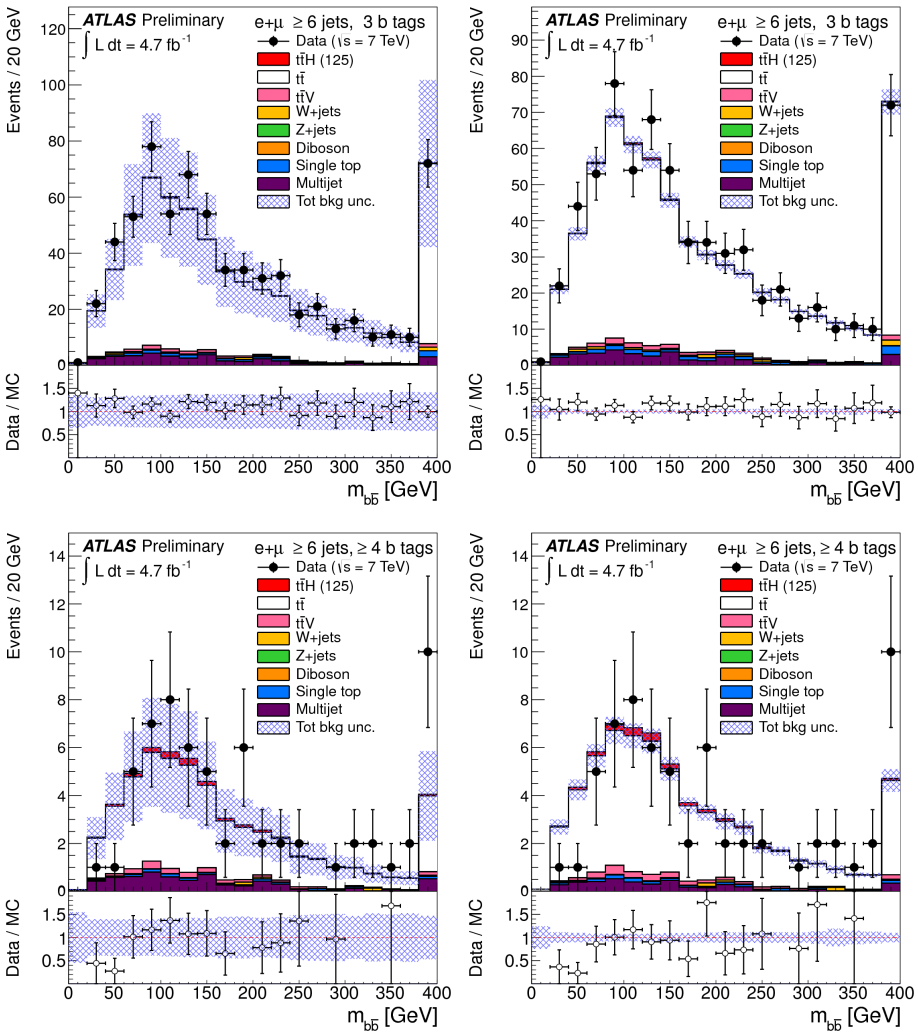

Figure 5: The reconstructed $m_{\tau\tau}$ distribution, as calculated by the missing mass calculator technique, in two event categories used in the $H \to \tau^+\tau^-$ search, taken from reference [14].

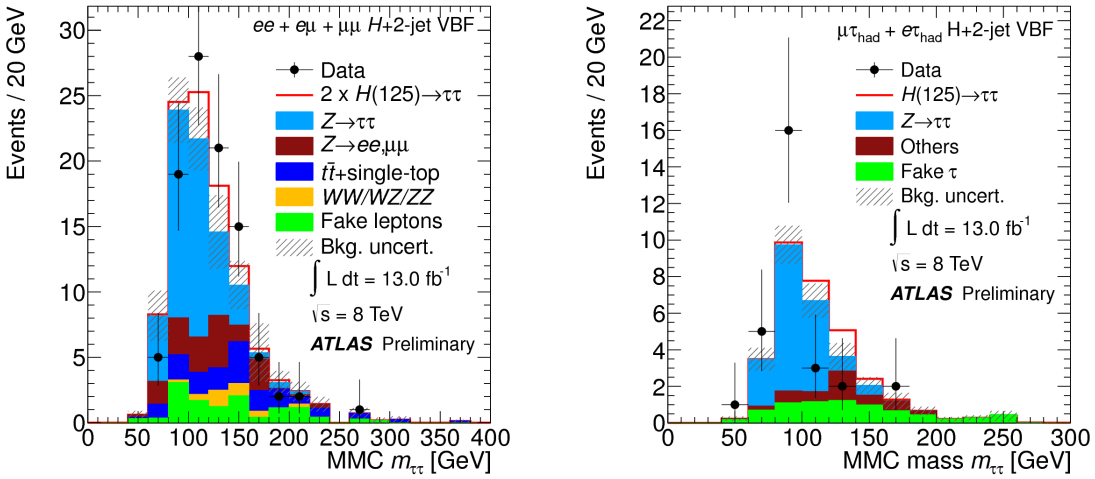

6 Searches for $H \to \tau^+\tau^-$ production

The search for $H \to \tau^+\tau^-$ at ATLAS [14] uses 4.6 fb^{-1} of data at $\sqrt{s} = 7$ TeV and 13.0 fb^{-1} of data at $\sqrt{s} = 8$ TeV. The search uses around ten exclusive analysis categories. The event categories are defined using the final states of the two τ-leptons, the number of additional jets and kinematic features. The different categories are optimised to be sensitive to different Higgs boson production mechanisms including Higgs boson production through vector boson fusion (VBF), "boosted" Higgs boson production (where the Higgs boson has a large momentum boost in the transverse plane) and associated production with a W- or Z-boson. In all categories, the di-τ invariant mass, $m_{\tau\tau}$, is used as the discriminating variable.

The variable $m_{\tau\tau}$ is reconstructed using the missing mass calculator technique [15] which takes into account the measured momentum, the measured missing transverse momentum, $E_{\mathrm{T}}^{\mathrm{miss}}$, and the simulated distribution of angle between visible and missing momenta.

The most sensitive category in the search is the $H \to \tau_{\mathrm{had}}\tau_{\mathrm{lep}}$ VBF category. In addition to the $H \to \tau_{\mathrm{had}}\tau_{\mathrm{lep}}$ candidate, this category requires two additional forwards jets with a high rapidity gap ($\Delta\eta > 3$). This category of events is particularly sensitive to Higgs boson production via vector-boson fusion. Figure 5 shows the reconstructed $m_{\tau\tau}$ distribution in some of the VBF search categories.

6.1 Backgrounds and Systematic Uncertainties

The main background to the search for $H \to \tau^+\tau^-$ production is due to $Z \to \tau^+\tau^-$ production. This background is studied using a data-driven technique. Measured $Z \to \mu^+\mu^-$ events are used, with the muons replaced by τ-lepton decay signatures taken from simulation. Further background contributions come from $Z \to \ell^+\ell^-$ + jet production, top-quark production and di-boson production. Each of these backgrounds are estimated from Monte Carlo samples, with corrections from data. QCD multi-jet production is estimated using a data-driven technique.

The main systematic uncertainties are due to the knowledge of the τ-lepton energy scale and from theoretical uncertainties.

6.2 $H \to \tau^+\tau^-$ Production Properties

The results of the search are interpreted as an observation of $H \to \tau^+\tau^-$ production, and shown in Figure 6. As the different categories involved in the search are sensitive to different

Figure 6: Results from the $H \to \tau^+\tau^-$ search, taken from reference [14]. Left: The observed and expected local p_0 values as a function of the Higgs boson mass. The dashed blue line is the expected p_0 for the value of the Higgs boson on the x-axis. The dotted magenta line shows the expected p_0 calculated for a Higgs boson signal with $m_H = 125$ GeV. Right: Likelihood contours in the ($\mu_{ggF} \times B/B_{SM}$, $\mu_{VBF+VH} \times B/B_{SM}$) plane for 68% and 95% confidence levels. The Standard Model expectation and expectation for background only is also shown.

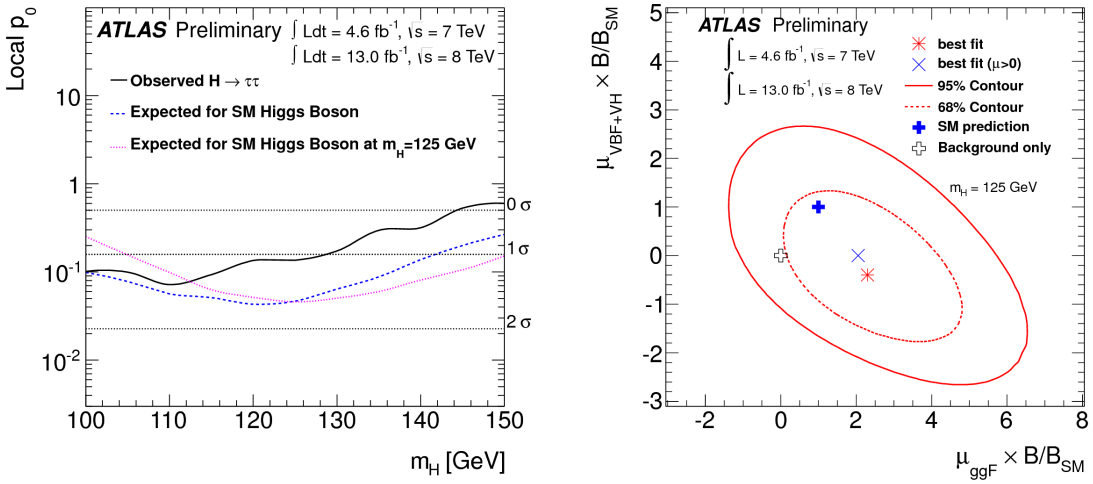

Higgs boson production modes, a measurement is also made of the strength of the Higgs boson production cross section in association with vector bosons (vector boson fusion and associated production with W- and Z-bosons) versus direct Higgs boson production from gluon fusion for $m_H = 125$ GeV. The results are also shown in Figure 6 and are consistent with Standard Model expectations.

As no significant excess above background predictions was observed, a measured (expected) limit is set on $\sigma(H \to \tau^+\tau^-)/\sigma_{SM}$ at 95% confidence level of 1.9 (1.2).

7 Searches for $H \to \mu^+\mu^-$ Production

Using 20.7 fb^{-1} of pp collision data at $\sqrt{s} = 8$ TeV, a search was performed for $H \to \mu^+\mu^-$ production [16]. The main background to this search is from Drell-Yan production $Z/\gamma^* \to \mu^+\mu^-$. Studies of simulated data were used to determine the resolution with which ATLAS could reconstruct a narrow di-muon resonance. For a decay of a 125 GeV object into muons, the resolution would be 2.3 GeV. As shown in Figure 7, no significant observation above the Standard Model backgrounds is observed and therefore a 95% confidence level limit is set on σ/σ_{SM} for $m_H = 125$ GeV of 9.8 measured (8.2 expected). The limits as a function of m_H are shown in Figure 8.

8 Summary and Outlook

No evidence for Standard Model Higgs boson production, decaying into fermion or invisible final states has been observed in the range 100 GeV $< m_H <$ 150 GeV. However, given the amount of data analysed in these searches, no observation was expected. The results are summarised in Table 4 and in Figure 8.

The study of the full 21 fb^{-1} dataset collected by ATLAS in 2012 is underway for the $VH \to Vb\bar{b}$, $t\bar{t}H, H \to b\bar{b}$ and $H \to \tau^+\tau^-$ searches. Further sensitivity to Higgs bosons production into leptons can be achieved by adding further final states, such as $t\bar{t}H \to \ell^+\nu b\,\ell^-\bar{\nu}b\,b\bar{b}$, and with a better understanding of flavour tagging and tau reconstruction. In addition, using advanced data-driven techniques to understand systematic uncertainties and gain better sep-

Figure 7: The invariant di-muon mass distribution used in the search for $H \to \mu^+\mu^-$ production; also shown are the estimated contributions from the signal and Standard Model backgrounds, and the ratio between data and Standard Model predictions, taken from reference [16].

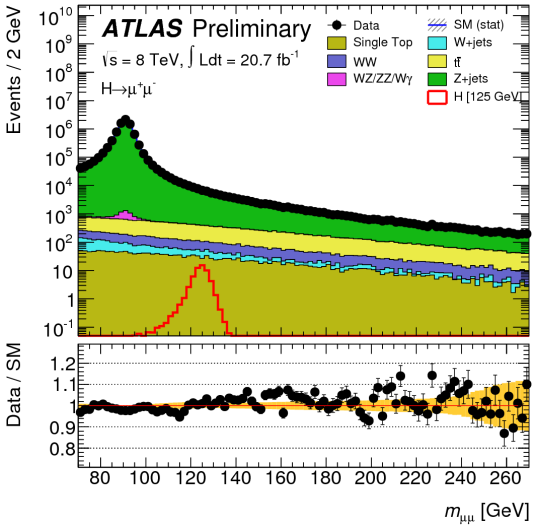

Figure 8: The observed and expected limits on Higgs boson production as a function of m_H for each of the searches presented in these proceedings [11,13,14,16]. In each plot, the solid black line represents the observed limit, the dashed line represents the expected limit and the coloured bands represent the $\pm 1\sigma$ and $\pm 2\sigma$ uncertainties on the expected limit.

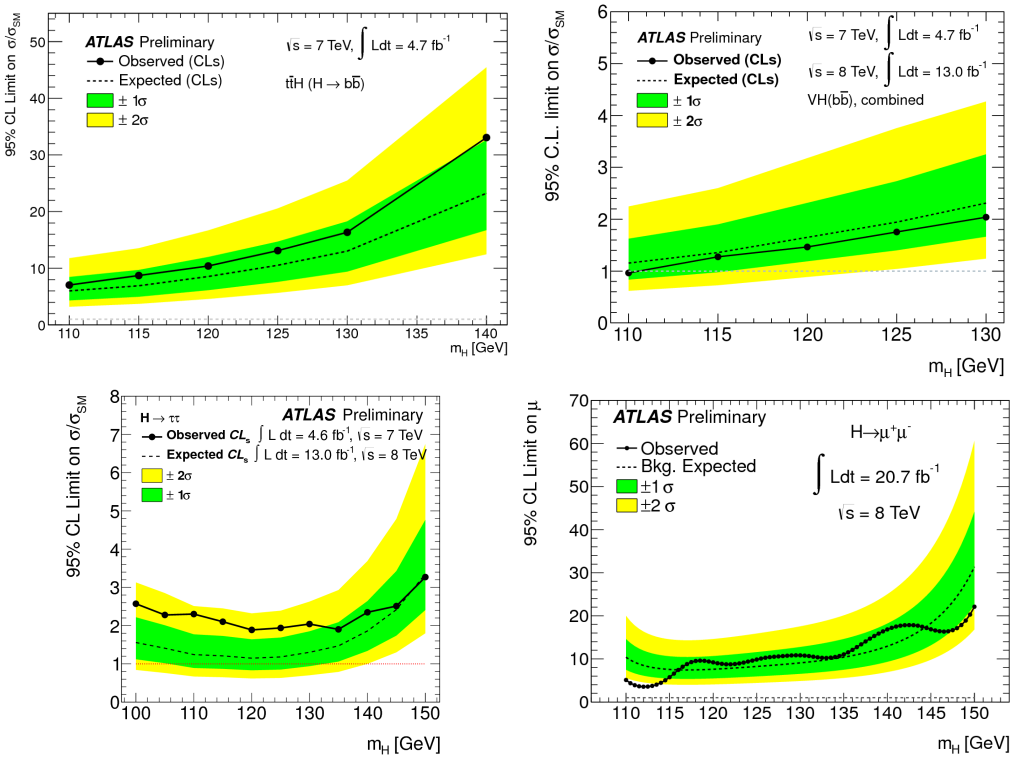

Table 4: Summary of ATLAS searches from Higgs boson decays into fermions [11,12,13,14,16]. Left: 95% CL limits on Higgs boson production for $m_H = 125$ GeV on $\sigma/\sigma_{\rm SM}$. Right: 95% CL limits on Higgs boson branching ratios for $m_H = 125$ GeV.

	observed	expected
$VH, H \to b\bar{b}$	1.8	1.9
$t\bar{t}H, H \to b\bar{b}$	13.1	10.5
$H \to \tau^+\tau^-$	1.9	1.2
$H \to \mu^+\mu^-$	9.8	8.2

	observed	expected
$H \to$ invisible	$< 65\%$	$< 84\%$

aration between signal and background will help improve sensitivity. At ATLAS studies are underway to use multivariate event selection, exploiting b-jet likelihoods and using kinematic fits of the observed final states.

The very small Higgs boson production cross section and the huge backgrounds at the LHC make Higgs boson searches into leptons very challenging. If the Higgs-like boson with $m_H \sim 125$ GeV is indeed the Standard Model Higgs boson, data from the post-LHC-shutdown period will be required to finally determine the Yukawa couplings [17].

Acknowledgments

The author acknowledges support for her work and for travel to the conference from the Science and Technologies Facilities Council of the United Kingdom and the help, support, hard work and dedication of her ATLAS colleagues in producing the results for, and helping with the preparation of, these proceedings and the associated presentation. The author also thanks the organisers of the conference for a very interesting and stimulating week.

References

1. F. Englert, R. Brout, *Phys. Rev. Lett.* **13**, 321 (1964).
2. P.W. Higgs, *Phys. Rev. Lett.* **13**, 508 (1964).
3. P.W. Higgs, *Phys. Lett.* **12**, 132 (1964).
4. G. Guralnik, C. Hagen, T. Kibble, *Phys. Rev. Lett.* **13**, 585 (1964).
5. The ATLAS Collaboration, *JINST* **3**, S08003 (2008).
6. The ATLAS Collaboration, *Phys. Lett.* B **716**, 1 (2012).
7. The CMS Collaboration, *Phys. Lett.* B **716**, 30 (2012).
8. The CDF and DØ Collaborations, PRL **109**, 071804 (2012)
9. LHC Higgs Cross Section Working Group, CERN-2011-002, http://arxiv.org/abs/1101.0593.
10. ATLAS Collaboration, ATLAS-CONF-2012-040, http://cds.cern.ch/record/1435194; ATLAS-CONF-2012-043, http://cds.cern.ch/record/1435197; ATLAS-CONF-2012-097, http://cds.cern.ch/record/1460443; ATLAS-CONF-2012-142, http://cds.cern.ch/record/1485531.
11. ATLAS Collaboration, ATLAS-CONF-2012-161, http://cds.cern.ch/record/1493625.
12. ATLAS Collaboration, ATLAS-CONF-2013-011, http://cds.cern.ch/record/1523696.
13. ATLAS Collaboration, ATLAS-CONF-2012-135, http://cds.cern.ch/record/1478423.
14. ATLAS Collaboration, ATLAS-CONF-2012-160, http://cds.cern.ch/record/1493624.
15. A. Elagin, P. Murat, A. Pranko and A. Safonov, *Nucl. Instrum. Methods* A **654**, 481 (2011). http://arxiv.org/abs/1012.4686
16. ATLAS Collaboration, ATLAS-CONF-2013-010, http://cds.cern.ch/record/1523695.
17. ATLAS Collaboration, ATL-PHYS-PUB-2012-004, http://cds.cern.ch/record/1484890.